

Water-soluble phosphorus porphyrins with high activity for visible light-assisted inactivation of *Saccharomyces cerevisiae*

Jin Matsumoto^a, Tomohiko Shinbara^a, Shin-ichiro Tanimura^a, Tomoko Matsumoto^a,
Tsutomu Shiragami^a, Haruhiko Yokoi^a, Yoshio Nosaka^b, Shigetoshi Okazaki^c,
Kazutaka Hirakawa^d, Masahide Yasuda^{a,*}

^a Department of Applied Chemistry, Faculty of Engineering, University of Miyazaki, Gakuen-Kibanadai, Miyazaki 889-2192, Japan

^b Department of Materials Science and Technology, Nagaoka University of Technology, Kamitomiokamachi 1603-1, Nagaoka, Niigata 940-2188, Japan

^c Photon Medical Research Center, Hamamatsu University School of Medicine, Handayama 1-20-1, Higashi-ku, Hamamatsu, Shizuoka 431-3192, Japan

^d Department of Basic Engineering (Chemistry), Faculty of Engineering, Shizuoka University, Johoku 3-5-1, Naka-ku, Hamamatsu, Shizuoka 432-8561, Japan

ARTICLE INFO

Article history:

Received 18 September 2010

Received in revised form 3 December 2010

Accepted 4 January 2011

Available online 6 January 2011

Keywords:

Adsorption

Confocal laser scanning microscope

Water-soluble

Oil-soluble

Singlet oxygen

Ethylene glycol

Saccharomyces cerevisiae

ABSTRACT

In an effort to develop water-soluble singlet-oxygen ($^1\text{O}_2$) photosensitizer, we synthesized a series of phosphorus porphyrin complexes (**1**, $(\text{RO})_2\text{P}(\text{tpp})^+\text{Cl}^-$, tpp = tetraphenylporphyrinato ligand, $\text{R} = -(\text{CH}_2\text{CH}_2\text{O})_m-(\text{CH}_2)_n-\text{H}$, $m = 0-3$, $n = 1, 2, 4, 6$) and evaluated their performance characteristics. Water-solubilities of **1** ($m = 1, 2$ and $n = 1, 2, 4, 6$) were determined to be >1.0 mM, which was higher than the parent $(\text{HO})_2\text{P}(\text{tpp})^+\text{Cl}^-$. The quantum yields for the generation of $^1\text{O}_2$ in water based on the amount of $^1\text{I}^*$ were determined to be 0.73, 0.69, and 0.62 for **1d** ($m = 2, n = 4$), **1e** ($m = 2, n = 2$), and **1f** ($m = 2, n = 1$), respectively. Photo-inactivation by **1** was performed with yeast (*Saccharomyces cerevisiae*), and was evaluated using an inactivation factor $A_F = ([\text{1}]_M \times T_{1/2})^{-1}$, where $[\text{1}]_M$ is the minimum effective concentration of **1** and $T_{1/2}$ is a half-life of the yeast initially used. In the case of **1b** ($m = 1, n = 6$) and **1c** ($m = 2, n = 6$), $[\text{1}]_M$ was determined to be 5 nM in the photo-sterilization. Bio-affinity was evaluated by the adsorbed concentration of **1** ($[\text{P}]_{\text{ad}}$) into the yeast, which was measured by absorption spectrophotometry using a confocal laser-scanning microscope. These findings revealed that a large amount of **1** was adsorbed into the yeast. The estimated amount of **1b** obtained from 10 μM aqueous solution came to 171 mM (17,100 fold) in terms of concentration. As an increase in carbon number (n) of the alkyl group on axial ligands, A_F and $[\text{P}]_{\text{ad}}$ increased. It is strongly suggested that the photo-inactivation took place with the assistance of the attack of $^1\text{O}_2$ inside the cells.

© 2011 Elsevier B.V. All rights reserved.

1. Introduction

Much attention has been paid to singlet-oxygen photosensitizers ($^1\text{O}_2$ -sensitizers) which can be used in an aqueous solution in connection with photodynamic therapy [1]. Porphyrins and metalloporphyrins are an attractive candidate (e.g. photofrin[®]) because of their strong absorption band in the visible-light region [2]. However, porphyrin and metalloporphyrins are, in general, poorly water-soluble. Therefore, water-solubilization of porphyrins is achieved by an introduction of an ionic group such as ammonium [3], pyridinium [4], sulfonate [5], phosphonium [6] or carboxyl [2], to porphyrin ring. Some ionic water-soluble porphyrins have been applied to the photochemical inactivation of microorganism [4,7,8]. However, little is known whether these porphyrins operate on the surface or inside cells for inactivation. If the $^1\text{O}_2$ -sensitizer

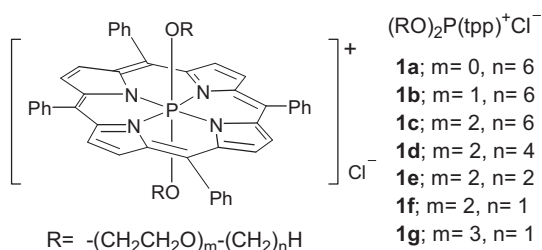
is effectively adsorbed inside the cell, it is expected that the $^1\text{O}_2$ -sensitizer will be more effective for photochemical inactivation of microorganisms. Here, we will elucidate their adsorption behavior and visible light-assisted inactivation of water-soluble di(polyoxaalkyl)tetraphenylporphyrinatophosphorus(V) chloride (**1**, $(\text{RO})_2\text{P}(\text{tpp})^+\text{Cl}^-$, $\text{R} = -(\text{CH}_2\text{CH}_2\text{O})_m-(\text{CH}_2)_n-\text{H}$, tpp = tetraphenylporphyrinato) to yeast (*Saccharomyces cerevisiae*) (Scheme 1).

2. Experimental

2.1. Instruments

^1H NMR (400 MHz) and ^{13}C NMR (100 MHz) spectra were taken with a Bruker AV 400 M spectrometer for CDCl_3 solutions using SiMe_4 as an internal standard. Matrix-assisted laser desorption/ionization mass spectra (MALDI-MS) were measured on a Bruker Daltonics Autoflex III TOF/TOF in the positive

* Corresponding author. Tel.: +81 985 58 7314; fax: +81 985 58 7315.
E-mail address: yasuda@cc.miyazaki-u.ac.jp (M. Yasuda).



Scheme 1. Water-soluble porphyrins (**1**).

ion mode at the Cooperative Research Center, University of Miyazaki.

Microscopic spectrophotometry was performed with an Olympus FV-300 confocal laser scanning microscope (CLSM) equipped with a spectrophotometer (STFL 250, Seki Technotron) linked to a CLSM with an optical fiber. The molar absorption coefficient (ϵ) of **1** at the Soret and Q bands were determined from the visible spectra measured in MeOH and an aqueous solution with a Shimadzu V-550 spectrophotometer.

2.2. Materials

The preparation of **1** was performed by the ligand-exchange of dichloro(tetraphenylporphyrinato)phosphorus chloride ($Cl_2P(tpp)^+Cl^-$) with 1-alkanol. The preparation of **1d** was the typical procedure. The **1d** was prepared by the heating of an MeCN (20 cm³) solution of $Cl_2P(tpp)^+Cl^-$ (75 mg) with 3,6-dioxadecanol (10 cm³) in the presence of small amounts of pyridine (10 drops) at reflux temperature for about 24 h until the Soret band shifted from 436 nm to 423 nm. The general follow-up procedure was as follows: After evaporation, the residue was dissolved into $CHCl_3$ (20 cm³). The $CHCl_3$ solution was washed three times with an aqueous solution (20 cm³). Here water-soluble **1** did not move from the $CHCl_3$ -phase to the water-phase at all. The washed $CHCl_3$ solution was subjected to reprecipitation with hexane (200 cm³) to remove the residual alkanol and other impurities. Moreover, the resulting precipitate was purified by column chromatography on SiO_2 using $CHCl_3$ –MeOH (100:1–30:1 v/v). The purity of **1** was confirmed by ¹H NMR spectra.

2.2.1. Di(hexyloxo)tetraphenylporphyrinatophosphorus(V) chloride (**1a**)

Yield 72%. ¹H NMR (400 MHz, $CDCl_3$) δ = –2.47 (dt, J = 12.4, 6.5 Hz, 4H), –1.59––1.52 (m, 4H), –0.93––0.86 (m, 4H), –0.09 (quint, J = 7.5 Hz, 4H), 0.30 (t, J = 7.5 Hz, 6H), 0.38 (sext, J = 7.5 Hz, 4H), 7.76–7.84 (m, 12H), 7.95–7.97 (m, 8H), 9.08 (d, J = 2.8 Hz, 8H); ¹³C NMR δ = 13.35, 21.45, 23.62, 27.07 (d, J = 16.1 Hz), 30.05, 61.45 (d, J = 16.3 Hz), 116.14 (d, J = 1.5 Hz), 128.46, 129.85, 133.05 (d, J = 5.1 Hz), 135.33, 139.13; UV–vis (MeOH) λ_{max}/nm ($\epsilon/10^4 M^{-1} cm^{-1}$) 429 (34.2), 560 (1.41), 601 (0.43); Exact mass (MALDI-MS) calcd. for $C_{56}H_{54}N_4O_2P$ [M^+]: 845.3984. Found: 845.3950.

2.2.2. Di(3-oxanonyloxo)tetraphenylporphyrinatophosphorus(V) chloride (**1b**)

Yield 55%. ¹H NMR (400 MHz, $CDCl_3$) δ = –2.27 (dt, J = 11.5, 5.6 Hz, 4H), 0.48–0.56 (m, 8H), 0.57–0.65 (m, 4H), 0.68 (t, J = 7.3 Hz, 6H), 0.78 (quint, J = 7.3 Hz, 4H), 0.92–1.02 (m, 4H), 2.02 (t, J = 6.6 Hz, 4H), 7.75–7.83 (m, 12H), 7.95–7.97 (m, 8H), 9.06 (d, J = 2.9 Hz, 8H); ¹³C NMR δ = 13.80, 22.26, 24.92, 28.43, 31.14, 60.60 (d, J = 15.4 Hz), 66.36 (d, J = 19.8 Hz), 70.18, 116.34 (d, J = 1.7 Hz), 128.42, 129.87, 133.08 (d, J = 5.5 Hz), 133.33, 135.25, 139.16; UV–vis (MeOH) λ_{max}/nm ($\epsilon/10^4 M^{-1} cm^{-1}$) 429 (24.9), 560 (1.21), 601 (0.33); Exact mass (MALDI-MS) calcd. for $C_{60}H_{62}N_4O_4P$ [M^+]: 933.4509. Found: 933.4480.

2.2.3. Di(3,6-dioxadodecyloxo)tetraphenylporphyrinatophosphorus(V) chloride (**1c**)

Yield 66%. ¹H NMR (400 MHz, $CDCl_3$) δ = –2.24 (dt, J = 11.8, 5.7 Hz, 4H), 0.55–0.58 (m, 4H), 0.80 (t, J = 7.1 Hz, 6H), 0.97–1.05 (m, 4H), 1.07–1.13 (m, 4H), 1.14–1.24 (m, 4H), 2.19–2.21 (m, 4H), 2.66–2.69 (m, 4H), 2.90 (t, J = 6.8 Hz, 4H), 7.76–7.83 (m, 12H), 7.96–7.98 (m, 8H), 9.06 (d, J = 2.9 Hz, 8H); ¹³C NMR δ = 13.92, 22.42, 25.41, 29.13, 31.44, 60.30 (d, J = 15.0 Hz), 66.90 (d, J = 19.8 Hz), 68.85, 69.24, 71.02, 116.30 (d, J = 1.5 Hz), 128.41, 129.84, 133.08 (d, J = 5.5 Hz), 133.33, 135.20, 139.15; UV–vis (MeOH) λ_{max}/nm ($\epsilon/10^4 M^{-1} cm^{-1}$) 429 (28.1), 560 (1.37), 601 (0.35); Exact mass (MALDI-MS) calcd. for $C_{64}H_{70}N_4O_6P$ [M^+]: 1021.5033. Found: 1021.4986.

2.2.4. Di(3,6-dioxadecyloxo)tetraphenylporphyrinatophosphorus(V) chloride (**1d**)

Yield 60%. ¹H NMR (400 MHz, $CDCl_3$) δ = –2.24 (dt, J = 11.8, 5.6 Hz, 4H), 0.57 (td, J = 5.6, 1.3 Hz, 4H), 0.72 (t, J = 7.3 Hz, 6H), 0.98–1.08 (m, 4H), 1.14–1.21 (m, 4H), 2.18–2.20 (m, 4H), 2.65–2.68 (m, 4H), 2.90 (t, J = 6.7 Hz, 4H), 7.75–7.83 (m, 12H), 7.96–7.98 (m, 8H), 9.06 (d, J = 2.9 Hz, 8H); ¹³C NMR δ = 13.78, 19.00, 31.31, 60.36 (d, J = 15.4 Hz), 66.97 (d, J = 20.0 Hz), 68.91, 69.33, 70.74, 116.36 (d, J = 1.3 Hz), 128.48, 129.90, 133.15 (d, J = 5.5 Hz), 133.40, 135.28, 139.22; UV–vis (MeOH) λ_{max}/nm ($\epsilon/10^4 M^{-1} cm^{-1}$) 429 (30.3), 560 (1.42), 601 (0.39); Exact mass (MALDI-MS) calcd. for $C_{60}H_{62}N_4O_6P$ [M^+]: 965.4407. Found: 965.4372.

2.2.5. Di(3,6-dioxaoctyloxo)tetraphenylporphyrinatophosphorus(V) chloride (**1e**)

Yield 59%. ¹H NMR (400 MHz, $CDCl_3$) δ = –2.23 (dt, J = 11.9, 5.7 Hz, 4H), 0.56 (td, J = 5.7, 1.4 Hz, 4H), 0.84 (t, J = 7.0 Hz, 6H), 2.19–2.21 (m, 4H), 2.68–2.70 (m, 4H), 2.98 (quint, J = 7.0 Hz, 4H), 7.76–7.83 (m, 12H), 7.96–7.98 (m, 8H), 9.06 (d, J = 2.9 Hz, 8H); ¹³C NMR δ = 14.72, 60.23 (d, J = 15.2 Hz), 66.10, 66.90 (d, J = 19.8 Hz), 68.60, 69.28, 116.29 (brs), 128.41, 129.85, 133.09 (d, J = 5.3 Hz), 133.32, 135.20, 139.15; UV–vis (MeOH) λ_{max}/nm ($\epsilon/10^4 M^{-1} cm^{-1}$) 429 (30.5), 560 (1.44), 601 (0.33); Exact mass (MALDI-MS) calcd. for $C_{56}H_{54}N_4O_6P$ [M^+]: 909.3781. Found: 909.3752.

2.2.6. Di(3,6-dioxahexyloxo)tetraphenylporphyrinatophosphorus(V) chloride (**1f**)

Yield 56%. ¹H NMR (400 MHz, $CDCl_3$) δ = –2.23 (dt, J = 11.9, 5.7 Hz, 4H), 0.55 (td, J = 5.7, 1.1 Hz, 4H), 2.19–2.21 (m, 4H), 2.65–2.67 (m, 4H), 2.87 (s, 6H), 7.76–7.83 (m, 12H), 7.96–7.98 (m, 8H), 9.06 (d, J = 2.9 Hz, 8H); ¹³C NMR δ = 58.49, 60.18 (d, J = 14.9 Hz), 66.91 (d, J = 19.8 Hz), 69.14, 70.75, 116.28 (d, J = 1.8 Hz), 128.41, 129.83, 133.08 (d, J = 5.5 Hz), 133.31, 135.17, 139.13; UV–vis (MeOH) λ_{max}/nm ($\epsilon/10^4 M^{-1} cm^{-1}$) 429 (28.2), 560 (1.40), 601 (0.37); Exact mass (MALDI-MS) calcd. for $C_{54}H_{50}N_4O_6P$ [M^+]: 881.3468. Found: 881.3480.

2.2.7. Di(3,6,9-trioxadecyloxo)tetraphenylporphyrinatophosphorus(V) chloride (**1g**)

Yield 67%. ¹H NMR (400 MHz, $CDCl_3$) δ = –2.25 (dt, J = 11.9, 5.7 Hz, 4H), 0.57 (td, J = 5.7, 1.5 Hz, 4H), 2.19–2.21 (m, 4H), 2.71–2.74 (m, 4H), 3.04–3.06 (m, 4H), 3.15 (s, 6H), 3.15–3.17 (m, 4H), 7.75–7.82 (m, 12H), 7.96–7.98 (m, 8H), 9.06 (d, J = 3.0 Hz, 8H); ¹³C NMR δ = 58.78, 60.32 (d, J = 15.8 Hz), 66.92 (d, J = 19.6 Hz), 69.10, 69.44, 69.91, 71.44, 116.34 (d, J = 1.5 Hz), 128.45, 129.88, 133.13 (d, J = 5.1 Hz), 133.38, 135.24, 139.19; UV–vis (MeOH) λ_{max}/nm ($\epsilon/10^4 M^{-1} cm^{-1}$) 429 (28.6), 560 (1.35), 601 (0.38); Exact mass (MALDI-MS) calcd. for $C_{58}H_{58}N_4O_8P$ [M^+]: 969.3992. Found: 969.4018.

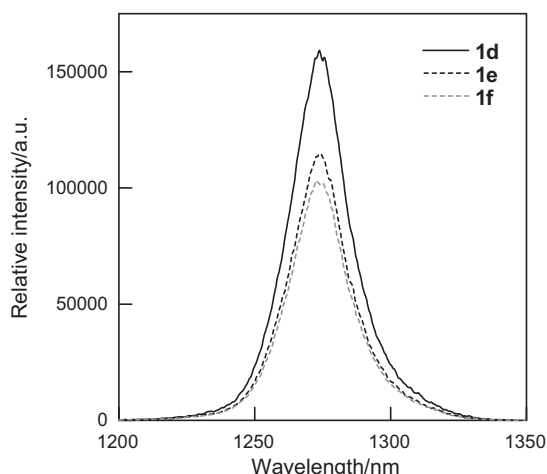


Fig. 1. Near-infrared luminescence spectra of $^1\text{O}_2$ around 1270 nm.

2.3. Water- and oil-solubilities

The solubility of **1** in water was defined as the saturated concentration (C_W) by the following method [9]. The C_W of **1** was measured with **1** (5 mg) suspended in pure water (1 cm^3) and left to stand for 3 days. A given volume of supernatant solution was moved to another vessel and diluted with MeOH to measure the absorption spectra of the solution. The C_W was calculated using absorbance and ε_{429} in MeOH. The solubility (C_0) of **1** in dioxane was determined in a similar manner to that used for C_W .

2.4. Determination of the quantum yields for the formation of $^1\text{O}_2$

The $^1\text{O}_2$ formation was directly measured by near-infrared luminescence around 1270 nm from deactivated $^1\text{O}_2$, which corresponds to the $^1\text{O}_2 (^1\Delta_g) \rightarrow ^3\text{O}_2 (^3\Sigma_g^-)$ transition (Fig. 1). The emission from $^1\text{O}_2$ was measured using an apparatus based on commercially available apparatuses and was improved for high-sensitivity detection (NIR-P11 System, Hamamatsu Photonics K.K., Hamamatsu, Japan). The excitation pulse was obtained using an optical parametric oscillator (OPO) (L5996, Hamamatsu Photonics K.K., Hamamatsu, Japan) excited by a Nd:YAG laser (Surelite I-20, Continuum, CA, USA). The excitation wavelength was 558 nm. Pulse width and intensity were approximately 7 ns and 500 $\mu\text{J}/\text{pulse}$, respectively, and the repetition rate was 20 Hz. Emission of $^1\text{O}_2$ was monitored using an infrared-gated image intensifier (NIR-

P11, Hamamatsu Photonics K.K., Hamamatsu, Japan) after passage through a polychromator (MS257, Oriel Instruments, CT, USA). Measurements started at 1 μs after application of the excitation pulse, and the exposure time was 100 μs . Signals were accumulated by repeated detection (2000 times). Calibration of the wavelength was performed using a spectral calibration lamp (Krypton type, Oriel Instruments, CT, USA). The quantum yields of $^1\text{O}_2$ formation were estimated from the comparison of the $^1\text{O}_2$ emission intensities by **1d–f** (20 μM) in a 2.0 cm^3 H_2O solution and methylene blue ($^1\text{O}_2$ quantum yield: 0.52 in H_2O) [10].

2.5. Determination of the T_1 lifetime by the time profile of $^1\text{O}_2$ emission

The excitation light was the second harmonic generator (532 nm) of a pulsed Nd:YAG laser (Continuum Minilite-II). The beam was passed through a set of dielectric multilayer film mirrors to eliminate stray light and irradiate from a 45° angle from the surface of a $1\text{ cm} \times 1\text{ cm} \times 4.5\text{ cm}$ quartz cell. Pulse width and intensity were approximately 5 ns and 2.9 mJ/pulse, respectively, and the repetition rate was 13 Hz. The emission of light from the front surface of the sample cell was collected with a set of quartz lenses, passed through a cold mirror (Sigma Koki, CLDM-50S), separated by a Bosch-Lomb Shimadzu monochromator, and then introduced into a photomultiplier (Hamamatsu, R5509-41), which was cooled to 200 K with liquid nitrogen. The signal from the photomultiplier was amplified by 75 with an amplifier (Stanford Research, SR-455) and then counted with a scaler/averager (Stanford Research, SR430). By changing the wavelength, the luminescence intensity showed a maximum at 1270 nm, confirming the detection of phosphorescence of $^1\text{O}_2$. For the time profile of $^1\text{O}_2$ emission, the signal obtained at 1270 nm was accumulated for 10,000 scans with a bin width of 40 ns, as shown in Fig. 2. The sample solution (2 cm^3 in 3.5 cm^3 quartz cell) containing **1d–f** (20 μM) in H_2O was measured with the above system. The emission intensity of $^1\text{O}_2$ at time t ($I(t)$) can be expressed with the following equation:

$$I(t) = A \left\{ \exp\left(-\frac{t}{\tau_d}\right) - \exp\left(-\frac{t}{\tau_r}\right) \right\} \quad (1)$$

where A is the preexponential factor, τ_d is the decay time of the emission, and τ_r is the rise of this emission [11]. When the lifetime of $^1\text{O}_2$ (τ_Δ) is longer than the lifetime of the T_1 state of the photosensitizer (τ_T), τ_d and τ_r equal τ_Δ and τ_T , respectively.

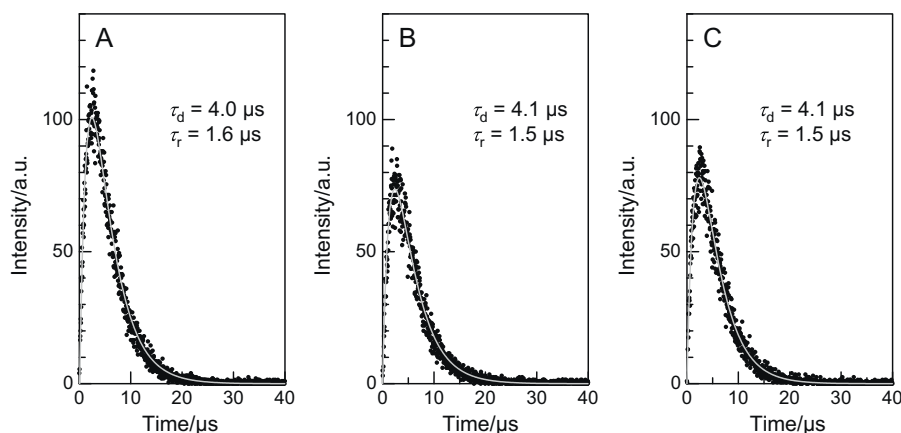


Fig. 2. The time profile of the near-infrared emission at ca. 1270 nm of $^1\text{O}_2$ generated by the photosensitized reaction of (A) **1d**, (B) **1e**, and (C) **1f**. The time constants, τ_d and τ_r , were calculated by fitting curve according to Eq. (1). Measurement conditions: number of laser pulses = 13 Hz, pulse duration = 5 ns, pulse energy = 2.9 mJ, the obtained time constants includes inherent errors within $\pm 0.1\text{ }\mu\text{s}$.

Table 1Photo-inactivation of yeast by **1** in an aqueous solution^a.

1 ([1] _M /nM) ^b	[NaCl]/wt%	Amount of cell [B]/10 ³ cell cm ^{-3c}							<i>T</i> _{1/2} ^d /min
		Time/min ^e = 0	20	40	60	80	100	120	
1b (5)	0	11.3	11.5	9.57	6.43	3.87	1.87	1.07	68.8
1c (5)	0	12.0	10.1	7.77	6.63	3.97	2.30	1.50	63.6
1d (50)	0 ^f	11.9	10.4	11.7	10.8	10.6	11.6	11.1	– ^g
	0 ^h	9.53	10.3	10.6	10.7	11.6	11.2	10.4	– ^g
	0	10.3	7.97	5.23	3.63	2.63	2.10	1.53	54.8
	0.30	10.2	4.97	2.20	1.37	0.53	0.20	0.13	29.1
	0.60	9.93	9.93	7.83	6.03	3.63	1.73	0.90	70.5
	0.90	9.03	8.43	5.83	2.07	1.03	0.27	0.07	50.6
1e (200)	0	10.7	7.43	3.27	0.63	0.17	0	0	30.9
	0.30	10.4	10.1	8.83	5.70	2.73	1.10	0.60	64.5
	0.60	12.8	12.5	4.97	1.20	0.90	0.53	0.17	39.5
	0.90	11.7	10.0	5.73	2.20	1.23	0.57	0.40	39.6
1f (300)	0	10.4	10.1	10.2	8.93	4.57	2.10	0.60	80.7
	0.30	11.2	10.4	6.80	4.33	1.83	0.63	0.27	52.4
	0.60	9.37	9.40	7.17	2.97	1.20	0.47	0.03	56.3
	0.90	10.0	8.20	8.43	6.13	3.63	1.97	1.03	67.8
1g (500)	0	10.7	11.2	6.43	2.93	0.27	0.10	0	23.3
	0.30	9.50	8.43	5.37	1.17	0.47	0.07	0.10	41.9
	0.60	9.77	10.0	8.53	6.87	5.80	3.60	2.07	85.9
	0.90	8.93	9.10	7.93	3.97	1.47	0.97	0.67	59.7

^a The sterilization was performed in an aqueous solution (10 cm³) containing yeast (1 × 10⁴ cell cm⁻³) with **1** by the irradiation of a fluorescent lamp (10.5 W cm⁻²).^b The values in parenthesis were the minimum concentration of **1** ([**1**]_M) used in nM.^c The amounts of yeast at a given irradiation time.^d *T*_{1/2} was the time required to be reduced to one-half its initial concentration.^e Irradiation time in min.^f Under dark conditions.^g Not determined.^h Irradiation was performed for an aqueous solution containing yeast with **1** under argon-saturated atmosphere.

2.6. Preparation of cell suspension

Yeast (*S. cerevisiae* NBRC 2044) was cultured aerobically at 30 °C for 8 h in a basal medium (pH 6.5) consisting of bactotryptone (10 g dm⁻³, Difco), yeast extract (5 g dm⁻³), and NaCl (10 g dm⁻³). After centrifugation of the cultured broth for 10 min, the harvested cells were washed and suspended in water to create a cell suspension. Cell numbers were measured with a hemocytometer and the amount of yeast in the suspension was adjusted to ca. 2.5 × 10⁵ cell cm⁻³.

2.7. Photo-inactivation of yeast

A cell suspension of yeast (1 cm³, ca. 10⁵ cell cm⁻³) and an aqueous solution of **1** (0.1 cm³, 0.5–50 μM), and water (8.9 cm³) were introduced into L-type glass tubes, resulting in the aqueous solution (10 cm³) containing yeast cells (1 × 10⁴ cell cm⁻³) and **1** (5–500 nM). Irradiation was performed by a fluorescent lamp (Panasonic FL-15ECW, λ = 400–723 nm, λ_{max} = 545 nm) on a reciprocal shaker in a manner similar to the reported method [12]. Light intensity was measured to be 6.3 W cm⁻² on the top of L-type glass tubes.

A portion (0.1 cm³) of the reaction mixture was taken at 20 min intervals and plated on an agar medium. The amount of living cells ([**B**]) was defined as the average number of the colonies of yeast which appeared after incubation for 36 h at 30 °C in three replicate plates. The results are shown Table 1.

2.8. CLSM-analysis of the concentration of **1** adsorbed on *S. cerevisiae*

The bio-affinity of **1** to yeast was examined by quantitative analysis of **1** incorporated into the yeast cells with a CLSM [13]. An aqueous solution of **1** (0.5 cm³, 50 μM) was added to the cell

suspension (1.0 cm³; ca. 2.5 × 10⁴ cell cm⁻³) of yeast, and then an aqueous solution of agar (1 wt%; 1.0 cm³) was added into the solution in order to stop the Brownian motion of cells during the CLSM analysis. Before losing fluidity, a portion of the prepared aqueous solution containing **1** (10 μM), yeast (ca. 1.0 × 10⁴ cell cm⁻³) and agar (0.4 wt%) was placed on a space (1 cm × 1 cm) surrounded by a silicone spacer (thickness 50 μm) put on a glass slide. The glass slide was set on the stage to be subjected to absorption spectrophotometry at the area whose diameter was restricted to be 1.42 μm by 60-fold objective lens on a CLSM. The absorbance (*A*) at the Q-band near 560 nm and diameter (*b*) of cell were measured from absorption spectra and fluorescence image, respectively.

3. Results and discussion

3.1. Water-soluble P-porphyrins

It is believed that the Sb(V)- and P(V)-porphyrins are water-soluble since they are cationic. However, water solubilities (*C*_W) of dihydroxo Sb- and P-porphyrins, (HO)₂M(tpp)⁺ (M = Sb and P), were still low. Recently, we have found that the *C*_W of Sb-porphyrins can be enhanced by an introduction of long alkyl axial ligands due to the formation of the aggregation [9]. For example, *C*_W of (C₆H₁₃O)(MeO)Sb(tpp)⁺Br⁻ (1.09 mM) was much higher than that of the parent (HO)₂Sb(tpp)⁺Br⁻ (0.08 mM). We prepared the (RO)₂P(tpp)⁺Cl⁻ (**1**) by the reaction of Cl₂P(tpp)⁺Cl⁻ with the corresponding ROH in MeCN in the presence of small amount of pyridine according to the preparation method of Sb-analog [14]. In the case of (C₆H₁₃O)₂P(tpp)⁺Cl⁻ (**1a**), however, the introduction of a hexyloxo group did not enhance the *C*_W: i.e. *C*_W of **1a** was still low (0.023 mM). Therefore, we attempted to enhance *C*_W by the introduction of a hydrophilic ethyleneoxy group (EO, –CH₂CH₂O–) to the axial ligands of **1a**. The resulting **1b** had a relatively high *C*_W (1.11 mM) compared to **1a**. When the carbon number (*n*) of the

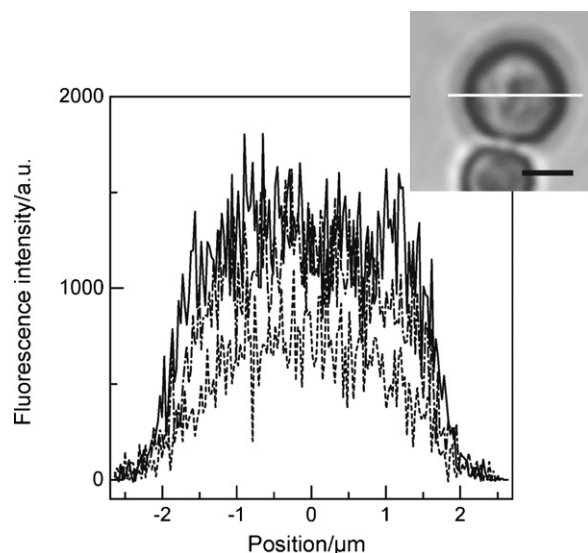


Fig. 3. Distribution of fluorescence intensity on the lines (white line) at the cross section at 0.3 (dotted line), 1.3 (dashed line), and 2.3 μm (solid line) depth from the uppermost yeast which was immersed in aqueous solution containing 10 μM of **1d** and 0.4 wt% of agar. The scale bar (black line) in inset is in 2 μm units.

alkyl group on $-(\text{EO})_2-(\text{CH}_2)_n\text{H}$ ligands decreased, the C_W values increased: $C_W = 2.07$ ($n=6$, **1c**), 5.38 ($n=4$; **1d**), 13.0 ($n=2$; **1e**), 13.9 mM ($n=1$; **1f**). The maximum C_W values were observed at **1g** ($m=3$, $n=1$), whose C_W was 17.3 mM. However, the C_O values of **1** were almost constant values, 0.140–0.293 mM, regardless of n and m . The C_W and C_O of **1** are summarized in Table 2.

3.2. Bio-affinity

As the microorganism, yeast was selected, because its size was sufficient for analysis by CLSM. The bio-affinity was evaluated by the adsorption experiment of **1** with yeast. An aqueous solution containing **1** (10 μM), yeast (ca. $1.0 \times 10^4 \text{ cell cm}^{-3}$) and agar (0.4 wt%) was placed on a glass slide. The glass slide was set on the stage to be subjected to absorption spectrophotometry with a CLSM. The distribution of the fluorescence intensity at a given cross-

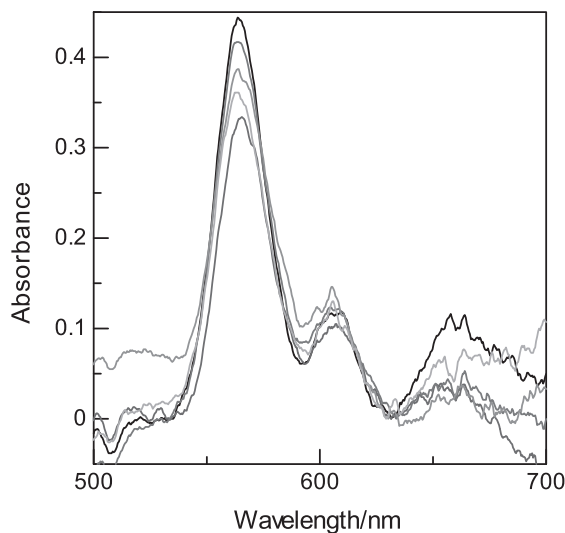


Fig. 4. The absorption spectra of Q-band of **1d** adsorbed in yeast which was immersed in aqueous solution containing 10 μM of **1d** and 0.4 wt% of agar. The $[P]_{\text{ad}}$ was determined to be $81.6 \pm 9.1 \text{ mM}$ using $b = 3.66 \pm 0.14 \mu\text{m}$ and $\epsilon_{560} = 1.30 \times 10^4 \text{ M}^{-1} \text{ cm}^{-1}$ according to $A = \epsilon_{560}b[P]_{\text{ad}}$.

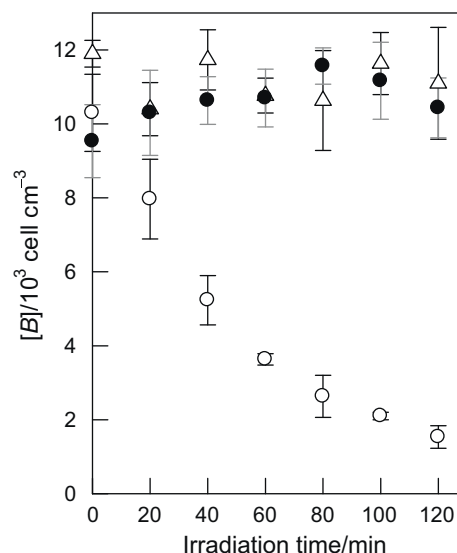


Fig. 5. Time-course plots of the visible-light assisted sterilization of yeast by **1d** under aerated conditions (○) and argon-saturated atmosphere (Δ). Dark reaction was performed in the presence of **1d** under aerated conditions (●).

section of cells shows the fluorescence came from inside rather than the walls of the cells, showing that **1** adsorbed inside cells (Fig. 3). The adsorbed concentration of **1** ($[P]_{\text{ad}}$) was analyzed by absorption spectrophotometry using molar absorption coefficient (ϵ_{560} ; Table 2), pathlength (b in cm), and absorbance (A), according to Lambert–Beer's law: $A = \epsilon_{560}b[P]_{\text{ad}}$ [13]. b was determined by the image of fluorescence emitted from the cells. A typical example of the absorption spectra of Q-band of **1d** adsorbed in yeast is shown in Fig. 4. The $[P]_{\text{ad}}$ values were determined by averaging $[P]_{\text{ad}}$ of five cells, as listed in Table 2. High amounts of **1b–f** were adsorbed into the yeast. For example, **1b** was concentrated into cells at 17,100 fold from 10 μM of an aqueous solution of **1b** to 171 mM. The $[P]_{\text{ad}}$ of **1g** with a large C_W was less than a measurable lower limit (1.65 mM). Thus, the large C_W trended to decrease $[P]_{\text{ad}}$. The adsorbed concentration of porphyrin derivatives on cells has been examined by MeOH-extraction method by Gupta et al. [15]. They have elucidated that the haematoporphyrin derivative (Photosan-3) was concentrated into human cerebral glioma cell (BGM-1) from ca. 17 μM of an aqueous solution to higher than 30 mM.

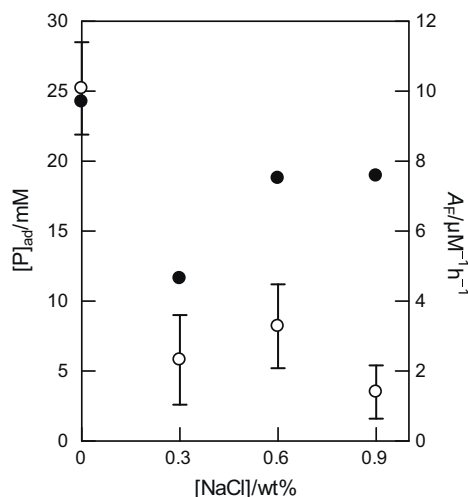


Fig. 6. Salt effect on the inactivation factor (A_f ; ●) and the adsorbed concentration of **1d** ($[P]_{\text{ad}}$; ○).

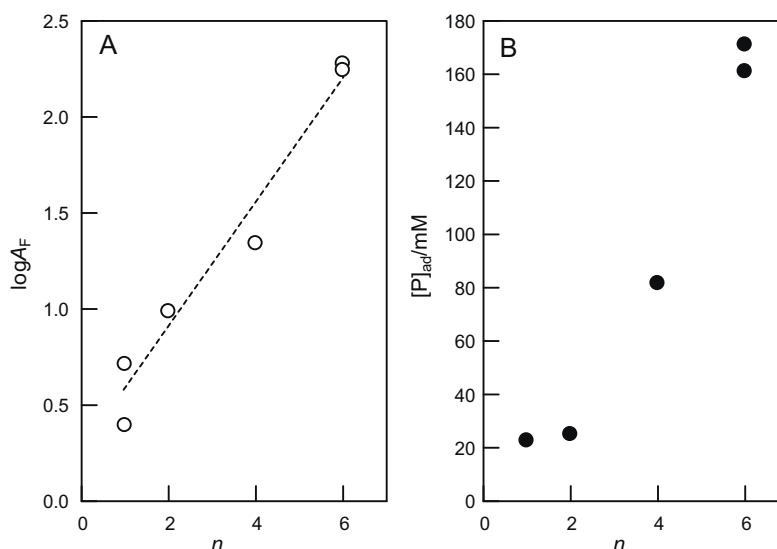


Fig. 7. Plots of (A) $\log A_F$ and (B) $[P]_{ad}$ vs. the carbon number (n) of the alkyl group on axial ligands.

3.3. Photochemical inactivation

Photochemical inactivation was performed for an aqueous solution (10 cm^3) of yeast ($1 \times 10^4 \text{ cell cm}^{-3}$) and **1** (5–500 nM) in an L-type tube under irradiation by a fluorescent lamp on a reciprocal shaker. A typical example of time course plots is shown in Fig. 5 from the case of **1d**. Under irradiated conditions, the amount of yeast ($[B]$) decreased exponentially from the initial concentration with an increase in irradiation time. In contrast, the control experiments in the presence of **1d** under dark conditions maintained $[B]$ at nearly original levels. Also, the photo-inactivation did not occur under argon-saturated atmosphere. From the time conversion, a half-life ($T_{1/2}$ in min), which is the time required to be reduced to one-half its initial concentration, was determined. The minimum effective concentrations of the **1** ($[1]_M$) were adjusted as $T_{1/2}$ became the values among 0–120 min. The $[1]_M$ varied between 5 and 500 nM, depending on the **1** used.

The treatment of microorganisms was usually performed in buffer solutions because many microorganisms cannot survive in pure water due to the higher osmotic pressure of the cells. However, the addition of salt lowered C_W of **1**. The additive effects of NaCl on bio-affinity and inactivation were examined for the case of

1e whose C_W was sufficiently high. As shown in Fig. 6, the $[P]_{ad}$ decreased with an increase in $[\text{NaCl}]$. However, A_F values were independent on $[\text{NaCl}]$.

3.4. Mechanism of inactivation reaction

Fig. 5 shows that the photo-inactivation under an argon-saturated atmosphere did not occur at all. Therefore, $^1\text{O}_2$ was responsible for the active species of the photo-inactivation [16]. Under visible-light irradiation, **1** was excited to singlet state to transform to triplet state with high efficiency. The energy transfer from the triplet state of **1** to $^3\text{O}_2$ molecules in a ground state took place to generate singlet oxygen ($^1\text{O}_2$). The overall quantum yields (Φ_Δ) for the generation of $^1\text{O}_2$ with **1** were determined in an aqueous solution to be 0.73 (**1d**), 0.69 (**1e**), and 0.62 (**1f**). These values were comparable values with other metalloporphyrins; 0.56 ($\text{H}_2(\text{tpp})$), 0.65 ($\text{Zn}(\text{tpp})$), and 0.62 ($\text{Mg}(\text{tpp})$) [17]. The lifetimes of T_1 of **1** were estimated from the time profile of $^1\text{O}_2$ emission and were determined to be 1.5–1.6 μs for **1d–1f**. The adsorption experiment showed that the aqueous solution of **1** ($10 \mu\text{M}$) was concentrated inside cells up to the $[P]_{ad}$ (22.6–171 mM). Thus, it is estimated that considerable amounts of **1** incorporated into cells diluted the con-

Table 2
Characterization of **1** and their bio-affinity ($[P]_{ad}$) and inactivation activity (A_F) towards yeast.

1	m	n	MW ^a	$\varepsilon_{560}/10^4 \text{ M}^{-1} \text{ cm}^{-1}$ ($\lambda_{\text{max}}/\text{nm}$) ^b	Φ_Δ ($\tau_T/\mu\text{s}$) ^c	Solubility ^d		Bio-affinity $[P]_{ad}/\text{mM}$ ^e	Inactivation		
						C_0/mM	C_W/mM		$[1]_M/\text{nM}$	$T_{1/2}/\text{min}$	$A_F/\mu\text{M}^{-1} \text{ h}^{-1}$
1a	0	6	881.5	1.41 (560) ^j	–	0.178	0.023	– ^j	–	–	– ^j
1b	1	6	969.6	1.01 (560)	–	0.242	1.11	171 ± 16	5	68.8	174.6
1c	2	6	1057.7	1.24 (561)	–	0.244	2.07	161 ± 15	5	63.6	188.7
1d	2	4	1001.6	1.30 (559)	0.73 (1.6)	0.293	5.38	81.6 ± 9.1	50	54.8	21.9
1e	2	2	945.5	1.44 (560)	0.69 (1.5)	0.169	13.0	25.0 ± 3.3	200	30.9	9.7
1f	2	1	917.4	1.40 (560)	0.62 (1.5)	0.140	13.9	22.6 ± 6.9	300	80.7	2.5
1g	3	1	1005.5	1.43 (560)	–	0.245	17.3	Nd ^k	500	23.3	5.2

^a Molecular weight.

^b Molar absorption coefficient of Q band in an aqueous solution. The values in parenthesis were the absorption maxima of the Q-band.

^c Quantum yields (Φ_Δ) for the formation of $^1\text{O}_2$ in an H_2O solution. The values in parenthesis were lifetime (τ_T) of triplet state of **1**.

^d C_W and C_0 were solubility in water and dioxane.

^e $[P]_{ad}$ was the concentration of **1** adsorbed into yeast which was immersed in $10 \mu\text{M}$ of aqueous solution of **1**.

^f $[1]_M$ was minimum effective concentration for photo-inactivation.

^g $T_{1/2}$ was the time required to be reduced to one-half its initial concentration.

^h $A_F = ([1]_M \times T_{1/2})^{-1}$.

ⁱ In MeOH solution.

^j $[P]_{ad}$ and A_F was not determined because of low C_W .

^k $[P]_{ad}$ was less than a measurable lower limit (1.65 mM).

centration of **1** (5–500 nM) of reaction conditions and operated as $^1\text{O}_2$ -sensitizer during its lifetime even under low O_2 pressure inside of cells.

The photo-inactivation was evaluated by the activity factor (A_F) which was derived from $[\mathbf{1}]_M$ and $T_{1/2}$: $A_F = ([\mathbf{1}]_M \times T_{1/2})^{-1}$. The $\log A_F$ and $[P]_{ad}$ were plotted against n , and showed a good relationship (Fig. 7). With an increase in n , the $\log A_F$ and $[P]_{ad}$ increased. As mentioned above, C_W values decreased as n increased. The C_O and C_W related the distribution ratio between oil- and water-phases. Since C_O values were almost constants, the **1** with a smaller C_W was favorable to distribute in oil-phases. Therefore, it can easily pass through the cell wall which consisted of hydrophobic peptideglucan, resulting in higher $[P]_{ad}$. Thus, the activity of **1** was mainly attributed to $[P]_{ad}$ because Φ_Δ was almost constant in **1**.

4. Conclusion

Recently, we found that the water-soluble dialkylxoantimony(V) tetraphenylporphyrin complex $(\text{RO})_2\text{Sb}(\text{tpp})^+$ shows bactericidal activity in 50 nM under visible-light irradiation [12]. Here, we successfully developed highly active $^1\text{O}_2$ -sensitizers (**1b** and **1c**) which operated in 5 nM for photo-inactivation of yeast. The high activity of **1b** and **1c** can be attributed to a higher $[P]_{ad}$. Long alkyl chains ($n=6$) took an advantage to interact with the hydrophobic cell wall. On the other hand, more than 1.0 mM of C_W was required to handle **1** in an aqueous solution because the **1** with a low C_W was adsorbed on the glassware. In the present case, the introduction of a few units of EO played a role in keeping more than 1.0 mM of C_W . Since P-porphyrins are light-element porphyrin, it is expected that **1** will be applicable to biological fields as a bio-degradable $^1\text{O}_2$ -sensitizer.

References

- [1] I.J. MacDonald, T.J. Dougherty, Basic principles of photodynamic therapy, J. Porphyrins Phthalocyanines 5 (2001) 105–129.
- [2] R.K. Pandey, G. Zheng, Porphyrins as photosensitizers in photodynamic therapy, in: Kadish, Smith, Guillard (Eds.), The Porphyrin Handbook, vol. 6, Academic Press, San Diego, 2000.
- [3] D.A. Caminos, M.B. Spesia, E.N. Durantini, Photodynamic inactivation of *Escherichia coli* by novel meso-substituted porphyrins by 4-(3-*N,N,N*-trimethylammoniumpropoxy)phenyl and 4-(trifluoromethyl)phenyl groups, Photochem. Photobiol. Sci. 5 (2006) 56–65.
- [4] K. Kano, M. Takei, S. Hashimoto, Cationic porphyrins in water. ^1H NMR and fluorescence studies on dimer and molecular complex formation, J. Phys. Chem. 94 (1990) 2181–2187.
- [5] X. Zhang, K. Sasaki, Y. Kuroda, Characterization of magnesium porphyrins and aggregation of porphyrins in organic solvent, Bull. Chem. Soc. Jpn. 80 (2007) 536–542.
- [6] R.-H. Jin, S. Aoki, K. Shima, Phosphoniumyl cationic porphyrins self-aggregation origin from π - π and cation- π interactions, J. Chem. Soc. Faraday Trans. 93 (1997) 3945–3953.
- [7] M. Salmon-Divon, Y. Nitzan, Z. Malik, Mechanistic aspects of *Escherichia coli* photodynamic inactivation by cationic tetra-meso(*N*-methylpyridyl)porphine, Photochem. Photobiol. Sci. 3 (2004) 423–429.
- [8] G.Y. Fraikin, M.G. Strakhovskaya, A.B. Rubin, The role of membrane-bound porphyrin-type compound as endogenous sensitizer in photodynamic damage to yeast plasma membranes, J. Photochem. Photobiol. B: Biol. 34 (1996) 129–135.
- [9] J. Matsumoto, S. Tanimura, T. Shiragami, M. Yasuda, Water-solubilization of alkylxo(methoxo)porphyrinatoantimony bromides, Phys. Chem. Chem. Phys. 11 (2009) 9766–9771.
- [10] Y.K. Usui, K. Kamogawa, A standard system to determine the quantum yield of singlet oxygen formation in aqueous solution, Photochem. Photobiol. 19 (1974) 245–247.
- [11] A.A. Krasnovsky Jr., Luminescence and photochemical studies of singlet oxygen photonics, J. Photochem. Photobiol. A 196 (2008) 210–218.
- [12] M. Yasuda, T. Nakahara, T. Matsumoto, T. Shiragami, J. Matsumoto, H. Yokoi, T. Hirano, K. Hirakawa, Visible light-assisted sterilization activity of water-soluble antimonyporphyrin toward *Saccharomyces cerevisiae*, J. Photochem. Photobiol. A 205 (2009) 210–214.
- [13] T. Matsumoto, T. Nakahara, J. Matsumoto, T. Shiragami, M. Yasuda, Quantitative analysis for water-soluble porphyrin derivatives adsorbed in *Saccharomyces cerevisiae* by absorption spectrophotometry using confocal laser scanning microscope, Bunseki Kagaku 58 (2009) 357–361.
- [14] T. Shiragami, K. Tanaka, Y. Andou, S. Tsunami, J. Matsumoto, H. Luo, Y. Araki, O. Ito, H. Inoue, M. Yasuda, Synthesis and spectroscopic analysis of tetraphenylporphyrinatoantimony(V) complexes linked to boron-dipyrin chromophore on axial ligands, J. Photochem. Photobiol. A: Chem. 170 (2005) 287–297.
- [15] S. Gupta, B.S. Dwarakanath, K. Muralidhar, V. Jain, Cellular uptake, localization and photodynamic effects of haematoporphyrin derivative in human glioma and squamous carcinoma cell lines, J. Photochem. Photobiol. B: Biol. 69 (2003) 107–120.
- [16] K. Hirakawa, S. Kawanishi, T. Hirano, H. Segawa, Guanine-specific DNA oxidation photosensitized by the tetraphenylporphyrin phosphorus(V) complex via singlet oxygen generation and electron transfer, J. Photochem. Photobiol. B: Biol. 87 (2007) 209–217.
- [17] C. Tanielian, C. Wolff, Porphyrin-sensitized generation of singlet molecular oxygen: comparison of steady-state and time-resolved methods, J. Phys. Chem. 99 (1995) 9825–9830.